

Axial couplings of heavy hadrons from domain-wall lattice QCD

William Detmold^{a,b}, C.-J. David Lin^{c,d}, Stefan Meinel^{*a}

^aDepartment of Physics, College of William & Mary, Williamsburg, VA 23187-8795, USA

^bJefferson Laboratory, 12000 Jefferson Avenue, Newport News, VA 23606, USA

^cInstitute of Physics, National Chiao-Tung University, Hsinchu 300, Taiwan

^dPhysics Division, National Centre for Theoretical Sciences, Hsinchu 300, Taiwan

E-mail: smeinel@wm.edu

We calculate matrix elements of the axial current for static-light mesons and baryons in lattice QCD with dynamical domain wall fermions. We use partially quenched heavy hadron chiral perturbation theory in a finite volume to extract the axial couplings g_1 , g_2 , and g_3 from the data. These axial couplings allow the prediction of strong decay rates and enter chiral extrapolations of most lattice results in the b sector. Our calculations are performed with two lattice spacings and with pion masses down to 227 MeV.

The XXIX International Symposium on Lattice Field Theory - Lattice 2011
July 10-16, 2011
Squaw Valley, Lake Tahoe, California

*Speaker.

1. Introduction

The low-energy dynamics of heavy-light mesons and baryons can be described by heavy-hadron chiral perturbation theory (HH χ PT), an effective field theory for QCD that incorporates both chiral symmetry and heavy-quark symmetry [1]. HH χ PT is essential for controlling light-quark-mass extrapolations of lattice QCD data in the heavy-quark sector (see for example Ref. [2]).

At leading order in the heavy-quark and chiral expansions, the HH χ PT Lagrangian contains three axial coupling constants that determine the strength of the interactions between heavy-light hadrons and pions: one coupling (denoted as g_1) for the heavy-light mesons, and two additional couplings (denoted as g_2, g_3) for the heavy-light baryons. These axial couplings are calculable from QCD, and their determination enables quantitative predictions for many heavy-light hadron properties (such as masses, decay widths, and various matrix elements) using HH χ PT. The chiral loop contributions that lead to the nonanalytic dependence of such properties on the light-quark masses are proportional to products of the relevant axial couplings. While g_1 has received much attention in the past because of its role for B mesons, the lesser-known couplings g_2 and g_3 are important for flavor physics with heavy baryons. The bottom baryon sector provides complementary information to B mesons for constraining the helicity structure of possible new physics [3].

The calculation of $g_{1,2,3}$ from the underlying theory of QCD must be done nonperturbatively, and hence on a lattice. The mesonic coupling g_1 had been studied previously in lattice QCD with $n_f = 0$ or $n_f = 2$ dynamical flavors [4]. In the following, we present a complete determination of all three axial couplings $g_{1,2,3}$ using $n_f = 2 + 1$ domain-wall lattice QCD [5, 6]. Our choice of lattice parameters (low pion masses, large volume, two lattice spacings) and our analysis method (fits to the axial-current matrix elements using the correct next-to-leading-order formulae from HH χ PT [7]) allow us to control all sources of systematic uncertainties.

2. Heavy-hadron chiral perturbation theory

We begin with an introduction to HH χ PT. This theory combines the chiral expansion with an expansion in powers of Λ_{QCD}/m_Q , where m_Q is the heavy-quark mass. We work at the leading order in the heavy-quark expansion, where the spin of the light degrees of freedom (s_l) is conserved and the heavy-quark spin decouples. The lowest-lying heavy-light mesons with $s_l = 1/2$ form multiplets with $J = 0$ and $J = 1$, which can be combined into a single field H^i :

$$H^i = [-P^i \gamma_5 + P_\mu^{*i} \gamma^\mu] \frac{1 - \not{v}}{2}, \quad \text{with} \quad (P^i) = \begin{pmatrix} B^+ \\ B^0 \end{pmatrix}, \quad (P^{*i})_\mu = \begin{pmatrix} B^{*+} \\ B^{*0} \end{pmatrix}_\mu. \quad (2.1)$$

(We consider $SU(2)$ HH χ PT and use the notation for bottom hadrons.) Similarly, the baryons with $s_l = 1$ form multiplets with $J = 1/2$ and $J = 3/2$. These are described by Dirac and Rarita-Schwinger fields B^{ij} and B_μ^{*ij} , which are symmetric in the flavor indices and can be combined into a single field S^{ij} :

$$S_\mu^{ij} = \sqrt{\frac{1}{3}} (\gamma_\mu + v_\mu) \gamma_5 B^{ij} + B_\mu^{*ij}, \quad \text{with} \quad (B^{ij}) = \begin{pmatrix} \Sigma_b^+ & \frac{1}{\sqrt{2}} \Sigma_b^0 \\ \frac{1}{\sqrt{2}} \Sigma_b^0 & \Sigma_b^- \end{pmatrix}, \quad (B^{*ij})_\mu = \begin{pmatrix} \Sigma_b^{*+} & \frac{1}{\sqrt{2}} \Sigma_b^{*0} \\ \frac{1}{\sqrt{2}} \Sigma_b^{*0} & \Sigma_b^{*-} \end{pmatrix}_\mu. \quad (2.2)$$

On the other hand, the $s_l = 0$ baryons ($J = 1/2$) are antisymmetric in flavor and include only the Λ_b in the $SU(2)$ case:

$$(T^{ij}) = \frac{1}{\sqrt{2}} \begin{pmatrix} 0 & \Lambda_b \\ -\Lambda_b & 0 \end{pmatrix}. \quad (2.3)$$

The leading-order HH χ PT Lagrangian, describing the interactions of the fields (2.1), (2.2), and (2.3) with pions, is given by

$$\begin{aligned} \mathcal{L} = & (\text{kinetic terms}) + g_1 \text{tr}_D [\bar{H}_i (\mathcal{A}^\mu)^i_j \gamma_\mu \gamma_5 H^j] \\ & - i g_2 \varepsilon_{\mu\nu\sigma\lambda} \bar{S}_{ki}^\mu v^\nu (\mathcal{A}^\sigma)^i_j (S^\lambda)^{jk} + \sqrt{2} g_3 [\bar{S}_{ki}^\mu (\mathcal{A}_\mu)^i_j T^{jk} + \bar{T}_{ki} (\mathcal{A}^\mu)^i_j S_\mu^{jk}]. \end{aligned} \quad (2.4)$$

In the terms with g_1 , g_2 , and g_3 , the pion field $\xi = \sqrt{\Sigma} = \exp(i\Phi/f)$ appears through

$$\mathcal{A}^\mu = \frac{i}{2} (\xi^\dagger \partial^\mu \xi - \xi \partial^\mu \xi^\dagger) = -\frac{1}{f} \partial^\mu \Phi + \dots, \quad (2.5)$$

which is an axial-vector field.

3. Axial current matrix elements

To determine the axial couplings g_i that appear in the chiral Lagrangian (2.4) from QCD, one can calculate suitable hadronic observables in both HH χ PT and lattice QCD. The expressions derived from HH χ PT are then fitted to the lattice data, and in these fits the axial couplings are parameters. The simplest observables that are sensitive to g_i are the zero-momentum matrix elements of the axial current between heavy-hadron states. In QCD, the isovector axial current is given by the quark current

$$A_\mu^{a(\text{QCD})} = \bar{q} \frac{\tau^a}{2} \gamma_\mu \gamma_5 q. \quad (3.1)$$

The corresponding hadronic current in HH χ PT can be obtained from the Lagrangian (2.4) using the Noether procedure. At leading order, the relevant part of the current that contributes to the matrix elements reads

$$\begin{aligned} A_\mu^{a(\chi\text{PT,LO})} = & g_1 \text{tr}_D [\bar{H}_i (\tau_{\xi+}^a)^i_j \gamma_\mu \gamma_5 H^j] - i g_2 \varepsilon_{\mu\nu\sigma\lambda} \bar{S}_{ki}^\nu v^\sigma (\tau_{\xi+}^a)^i_j (S^\lambda)^{jk} \\ & + \sqrt{2} g_3 [\bar{S}_{\mu ki} (\tau_{\xi+}^a)^i_j T^{jk} + \bar{T}_{ki} (\tau_{\xi+}^a)^i_j (S_\mu)^{jk}], \end{aligned} \quad (3.2)$$

with $\tau_{\xi+}^a = \frac{1}{2} (\xi^\dagger \tau^a \xi + \xi \tau^a \xi^\dagger)$. One finds the following matrix elements for $A_\mu = A_\mu^1 - i A_\mu^2$,

$$\begin{aligned} \langle P^{*d} | A_\mu | P^\mu \rangle &= -2 (g_1)_{\text{eff}} \varepsilon_\mu^*, \\ \langle S^{dd} | A_\mu | S^{du} \rangle &= -(i/\sqrt{2}) (g_2)_{\text{eff}} v^\sigma \varepsilon_{\sigma\mu\nu\rho} \bar{U}^\nu U^\rho, \\ \langle S^{dd} | A_\mu | T^{du} \rangle &= -(g_3)_{\text{eff}} \bar{U}_\mu \mathcal{U}, \end{aligned} \quad (3.3)$$

where ε^μ is the polarization vector of the P^{*d} meson and \mathcal{U} is the Dirac spinor of the T^{du} baryon. For the $s_l = 1$ baryons, we work directly with external S^{ij} states (which contain the degrees of freedom of both $J = 1/2$ and $J = 3/2$) and the U^μ 's are the corresponding generalized spinors [6]. At leading order in the chiral expansion, the “effective axial couplings” in (3.3) are equal to the

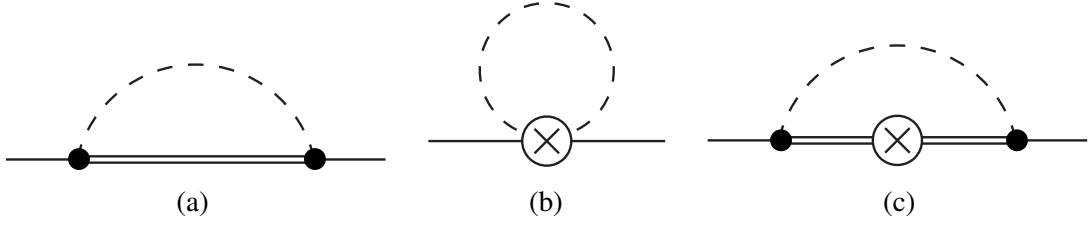


Figure 1: One-loop diagrams contributing to the matrix elements of the axial current in HH χ PT: (a) wavefunction renormalization diagram, (b) tadpole diagram, (c) sunset diagram [7].

axial couplings in the Lagrangian, $(g_i)_{\text{eff}}|_{\text{LO}} = g_i$. At next-to-leading order, the matrix elements receive corrections from pion loops (Fig. 1) and analytic counterterms. The NLO expressions for $(g_i)_{\text{eff}}$, both in the unquenched and the partially quenched theories, and for a finite volume, can be found in Ref. [7].

4. Lattice calculation

To calculate the matrix elements (3.3) in lattice QCD, we use the following interpolating fields for the heavy hadrons,

$$\begin{aligned} P^i &= (\gamma_5)_{\alpha\beta} \bar{Q}_{a\alpha} \tilde{q}_{a\beta}^i, & P_\mu^{*i} &= (\gamma_\mu)_{\alpha\beta} \bar{Q}_{a\alpha} \tilde{q}_{a\beta}^i, \\ S_\mu^{ij} &= \epsilon_{abc} (C\gamma_\mu)_{\beta\gamma} \tilde{q}_{a\beta}^i \tilde{q}_{b\gamma}^j Q_{c\alpha}, & T_\alpha^{ij} &= \epsilon_{abc} (C\gamma_5)_{\beta\gamma} \tilde{q}_{a\beta}^i \tilde{q}_{b\gamma}^j Q_{c\alpha}, \end{aligned} \quad (4.1)$$

where \tilde{q}^i denotes a smeared light-quark field of flavor i , and Q denotes the static heavy quark field (here we set $v = (1, 0, 0, 0)$). Just as in HH χ PT, the interpolating field S_μ^{ij} couples to both the $J = 1/2$ and $J = 3/2$ baryon states with $s_l = 1$. We use the domain-wall action [8] for the light quarks, and the Eichten-Hill action [9] with HYP-smeared temporal gauge links [10] for the heavy quarks. To optimize the signals and analyze heavy-quark discretization effects, we generated data for $n_{\text{HYP}} = 1, 2, 3, 5, 10$ levels of HYP smearing. The final results for the axial couplings are based on data with $n_{\text{HYP}} = 1, 2, 3$ only. The calculations are performed with the local 4-dimensional axial current, given by

$$A_\mu = Z_A \bar{d}_{a\alpha} (\gamma_\mu \gamma_5)_{\alpha\beta} u_{a\beta}, \quad (4.2)$$

where Z_A is determined nonperturbatively [11]. We compute the following ratios of three-point and two-point functions,

$$\begin{aligned} R_1(t, t') &= -\frac{1}{3} \frac{\sum_{\mu=1}^3 \langle P^{*d\mu}(t) A^\mu(t') P_u^\dagger(0) \rangle}{\langle P^u(t) P_u^\dagger(0) \rangle}, \\ R_2(t, t') &= i \frac{\sum_{\mu, \nu, \rho=1}^3 \epsilon_{0\mu\nu\rho} \langle S^{dd\mu}(t) A^\nu(t') \bar{S}_{du}^\rho(0) \rangle}{\sum_{\mu=1}^3 \langle S^{dd\mu}(t) \bar{S}_{dd}^\mu(0) \rangle}, \\ R_3(t, t') &= \left[\frac{1}{3} \frac{\sum_{\mu, \nu=1}^3 \langle S^{dd\mu}(t) A^\mu(t') \bar{T}_{du}(0) \rangle \langle T^{du}(t) A^{\nu\dagger}(t') \bar{S}_{dd}^\nu(0) \rangle}{\sum_{\mu=1}^3 \langle S^{dd\mu}(t) \bar{S}_{dd}^\mu(0) \rangle \langle T^{du}(t) \bar{T}_{du}(0) \rangle} \right]^{1/2}, \end{aligned} \quad (4.3)$$

where the source and sink hadron interpolating fields are placed at a common spatial point \mathbf{x} because of the static heavy quark, and we write $A^\mu(t') = \sum_{\mathbf{x}'} A^\mu(t', \mathbf{x}')$. In Eq. (4.3) we also removed

$L^3 \times T$	$am_{u/d}^{(\text{sea})}$	$am_{u/d}^{(\text{val})}$	a (fm)	$m_\pi^{(\text{vv})}$ (MeV)	$m_\pi^{(\text{vs})}$ (MeV)	values of t/a
$24^3 \times 64$	0.005	0.005	0.1119(17)	336(5)	336(5)	4, 5, 6, 7, 8, 9, 10
$24^3 \times 64$	0.005	0.002	0.1119(17)	270(4)	304(5)	4, 5, 6, 7, 8, 9, 10
$24^3 \times 64$	0.005	0.001	0.1119(17)	245(4)	294(5)	4, 5, 6, 7, 8, 9, 10
$32^3 \times 64$	0.006	0.006	0.0848(17)	352(7)	352(7)	13
$32^3 \times 64$	0.004	0.004	0.0849(12)	295(4)	295(4)	6, 9, 12
$32^3 \times 64$	0.004	0.002	0.0849(12)	227(3)	263(4)	6, 9, 12

Table 1: Lattice parameters. $m_\pi^{(\text{vv})}$ and $m_\pi^{(\text{vs})}$ denote the valence-valence and valence-sea pion masses.

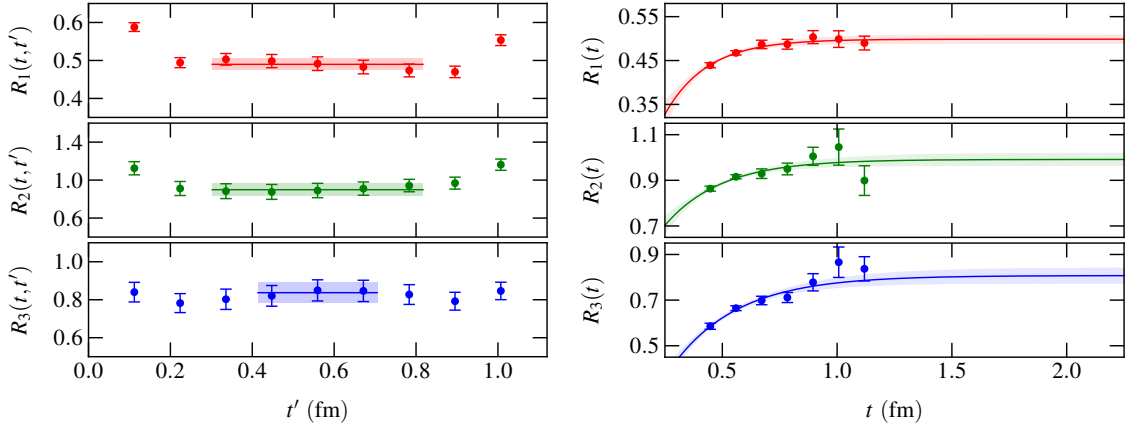


Figure 2: Left panel: ratios $R_i(t, t')$ for the source-sink separation $t/a = 10$, along with extracted values $R_i(t)$ (shaded regions). Right panel: extrapolation of $R_i(t)$ to infinite source-sink separation. All data shown here are for $a = 0.112$ fm, $am_{u,d}^{(\text{val})} = 0.002$, $n_{\text{HYP}} = 3$.

the free spinor indices which trivially originate from the static heavy-quark propagator. By inserting complete sets of states into (4.3), one can show that $R_i(t, t/2) = (g_i)_{\text{eff}} + \dots$, where the dots indicate contributions from excited states that decay exponentially with t [6].

Our calculations use RBC/UKQCD gauge field configurations with 2+1 dynamical quark flavors [11]. The main parameters of the ensembles and the domain-wall propagators we computed on them are given in Table 1. For the three-point functions we use pairs of light-quark propagators with sources at a common spatial point \mathbf{x} and separated by t/a steps in the time direction. As can be seen in the table, we have data for multiple values of t/a . Numerical examples for the ratios (4.3) are shown in Fig. 2 (left). Equivalently to using $R_i(t, t/2)$, we average $R_i(t, t')$ over t' in the central plateau regions, and we denote these averages as $R_i(t)$. We then perform fits of the form $R_i(t) = (g_i)_{\text{eff}} - A_i e^{-\delta_i t}$, as shown in Fig. 2 (right). A detailed discussion can be found in Ref. [6]. These fits provide the effective axial couplings $(g_i)_{\text{eff}}(a, m_\pi^{(\text{vv})}, m_\pi^{(\text{vs})}, n_{\text{HYP}})$ for all combinations of the lattice spacing, the pion masses, and the heavy-quark smearing parameter n_{HYP} . We fit the data for $(g_i)_{\text{eff}}(a, m_\pi^{(\text{vv})}, m_\pi^{(\text{vs})}, n_{\text{HYP}})$ with

$$(g_1)_{\text{eff}} = g_1 \left[1 + f_1(g_1, m_\pi^{(\text{vv})}, m_\pi^{(\text{vs})}, L) + c_1^{(\text{vv})} [m_\pi^{(\text{vv})}]^2 + c_1^{(\text{vs})} [m_\pi^{(\text{vs})}]^2 + d_{1, n_{\text{HYP}}} a^2 \right],$$

$$(g_i)_{\text{eff}} \Big|_{i=2,3} = g_i \left[1 + f_i(g_2, g_3, m_\pi^{(\text{vv})}, m_\pi^{(\text{vs})}, \Delta, L) + c_i^{(\text{vv})} [m_\pi^{(\text{vv})}]^2 + c_i^{(\text{vs})} [m_\pi^{(\text{vs})}]^2 + d_{i, n_{\text{HYP}}} a^2 \right], \quad (4.4)$$

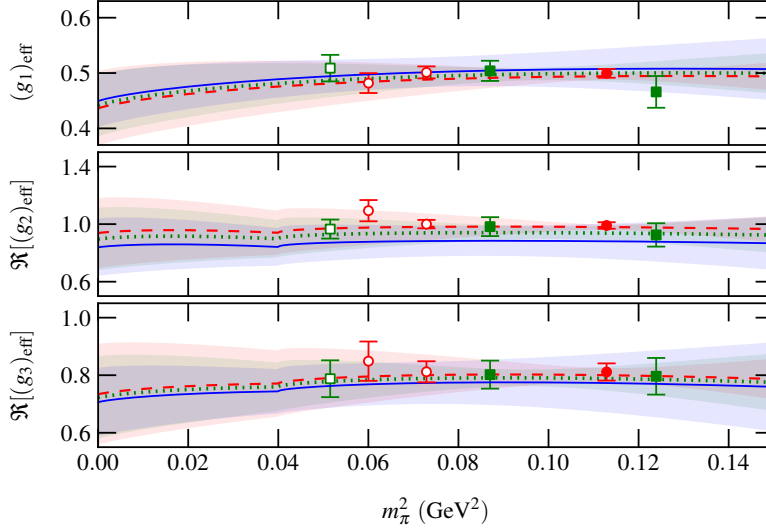


Figure 3: Fits of $(g_i)_{\text{eff}}$ using Eq. (4.4). The plot shows the fitted functions, evaluated at $m_\pi^{(\text{vv})} = m_\pi^{(\text{vs})} = m_\pi$ and in infinite volume, for $n_{\text{HYP}} = 3$. The baryonic matrix elements $(g_{2,3})_{\text{eff}}$ develop small imaginary parts below the $S \rightarrow T\pi$ decay threshold at $m_\pi = \Delta$, and only the real parts are shown here. The dashed line corresponds to $a = 0.112$ fm, the dotted line to $a = 0.085$ fm, and the solid line to the continuum limit. The $\pm 1\sigma$ regions are shaded. The data points (circles: $a = 0.112$ fm, squares: $a = 0.085$ fm) have been shifted to infinite volume for this plot, and the partially quenched data ($m_\pi^{(\text{vv})} < m_\pi^{(\text{vs})}$) are included using open symbols at $m_\pi = m_\pi^{(\text{vv})}$, even though the fit functions have slightly different values for these points.

where the functions f_i are the NLO loop contributions from $SU(4|2)$ HH χ PT, including the effects of the finite lattice size [5]. The terms with coefficients $c_i^{(\text{vv})}$ and $c_i^{(\text{vs})}$ are analytic NLO counterterms that cancel the renormalization-scale-dependence of f_i , and the terms with coefficients $d_{i,n_{\text{HYP}}}$ describe the leading effects of the non-zero lattice spacing. The functions $f_{2,3}$ also depend on the $S - T$ mass splitting Δ , which is included in the kinetic terms of Eq. (2.4). We set $\Delta = 200$ MeV, consistent with the $\Sigma_b^{(*)} - \Lambda_b$ splitting from experiment and with our lattice data.

To study the effect of the HYP smearing in the heavy-quark action on the scaling behavior, we performed initial fits that included all values of n_{HYP} , and then successively removed the data with the largest values of n_{HYP} . After excluding $n_{\text{HYP}} = 5, 10$, the fits were stable and had good Q -values. Our final results for the axial couplings are

$$\begin{aligned} g_1 &= 0.449 \pm 0.047_{\text{stat}} \pm 0.019_{\text{syst}}, \\ g_2 &= 0.84 \pm 0.20_{\text{stat}} \pm 0.04_{\text{syst}}, \\ g_3 &= 0.71 \pm 0.12_{\text{stat}} \pm 0.04_{\text{syst}}. \end{aligned} \quad (4.5)$$

The estimates of the systematic uncertainties in (4.5) include the effects of the following: NNLO terms in the fits to the a - and m_π -dependence (3.6%, 2.8%, 3.7% for g_1 , g_2 , g_3 , respectively), the above-physical value of the sea-strange-quark mass (1.5%), and higher excited states in $R_i(t)$ (1.7%, 2.8%, 4.9%). The details of the analysis can be found in Ref. [6].

Figure 3 shows the pion-mass dependence of the fitted functions $(g_i)_{\text{eff}}$. The counterterm parameters $c_i^{(\text{vv})}$ and $c_i^{(\text{vs})}$ resulting from the fits are natural-sized (for $\mu = 4\pi f_\pi$), and the NLO

contributions are significantly smaller than the LO contributions. We conclude that the $SU(4|2)$ chiral expansion of $(g_i)_{\text{eff}}$ convergences well for the pion masses used here.

5. Summary

We have calculated the heavy-hadron axial couplings using lattice QCD, including for the first time the baryonic couplings g_2 and g_3 in addition to the mesonic coupling g_1 . The analysis is based on data for the axial-current matrix elements at low pion masses, a large volume, and two different lattice spacings. We extracted $g_{1,2,3}$ from this data by performing chiral fits with the full NLO expressions from HH χ PT [7]. As a consequence, the systematic uncertainties in our results (4.5) are much smaller than the statistical uncertainties. The numerical values of $g_{1,2,3}$ can be used to constrain chiral fits of lattice QCD data for a wide range of heavy-light meson and baryon observables. Furthermore, our results for the axial couplings allow the direct calculation of certain observables in HH χ PT, in particular the strong decay widths of heavy baryons [5, 6].

Acknowledgments: WD is supported in part by JSA, LLC under DOE contract No. DE-AC05-06OR-23177 and by the Jeffress Memorial Trust, J-968. WD and SM are supported by DOE OJI Award DE-SC000-1784 and DOE grant DE-FG02-04ER41302. CJD is supported by NSC grant number 99-2112-M-009-004-MY3. We acknowledge the hospitality of Academia Sinica Taipei and NCTS Taiwan. This research made use of computational resources provided by NERSC and the NSF Teragrid.

References

- [1] M. B. Wise, Phys. Rev. D **45**, 2188 (1992); G. Burdman, J. F. Donoghue, Phys. Lett. B **280**, 287 (1992); T. M. Yan *et al.*, Phys. Rev. D **46**, 1148 (1992); P. L. Cho, Nucl. Phys. B **396**, 183 (1993).
- [2] A. S. Kronfeld, S. M. Ryan, Phys. Lett. B **543**, 59 (2002).
- [3] T. Mannel, S. Recksiegel, J. Phys. G **24**, 979 (1998).
- [4] G. M. de Divitiis *et al.* (UKQCD Collaboration), JHEP **10**, 010 (1998); A. Abada *et al.*, JHEP **0402**, 016 (2004); S. Negishi, H. Matsufuru, T. Onogi, Prog. Theor. Phys. **117**, 275 (2007); H. Ohki, H. Matsufuru, T. Onogi, Phys. Rev. D **77**, 094509 (2008); D. Bećirević *et al.*, Phys. Lett. B **679**, 231 (2009); J. Bulava, M. A. Donnellan, R. Sommer, PoS **LATTICE2010**, 303 (2010).
- [5] W. Detmold, C.-J. D. Lin, S. Meinel, arXiv:1109.2480.
- [6] W. Detmold, C.-J. D. Lin, S. Meinel, arXiv:1203.3378.
- [7] W. Detmold, C.-J. D. Lin, S. Meinel, Phys. Rev. D **84**, 094502 (2011).
- [8] D. B. Kaplan, Phys. Lett. B **288**, 342 (1992); Y. Shamir, Nucl. Phys. B **406**, 90 (1993); V. Furman, Y. Shamir, Nucl. Phys. B **439**, 54 (1995).
- [9] E. Eichten, B. R. Hill, Phys. Lett. B **240**, 193 (1990).
- [10] M. Della Morte *et al.* (ALPHA Collaboration), Phys. Lett. B **581**, 93 (2004).
- [11] Y. Aoki *et al.* (RBC/UKQCD Collaboration), Phys. Rev. D **83**, 074508 (2011).